Noname manuscript No.
(will be inserted by the editor)

A family of spatial biodiversity measures based on graphs

Tuomas Rajala · **Janine Illian**

the date of receipt and acceptance should be inserted later

Abstract While much research in ecology has focused on spatially explicit modelling as well as on measures of biodiversity, the concept of spatial (or local) biodiversity has been discussed very little. This paper generalises existing measures of spatial biodiversity and introduces a family of spatial biodiversity measures by flexibly defining the notion of the individuals' neighbourhood within the framework of graphs associated to a spatial point pattern. We consider two non-independent aspects of spatial biodiversity, scattering, i.e. the spatial arrangement of the individuals in the study area and exposure, the local diversity in an individual's neighbourhood.

A simulation study reveals that measures based on the most commonly used neighbourhood defined by the geometric graph do not distinguish well between scattering and exposure. This problem is much less pronounced when other graphs are used. In an analysis of the spatial diversity in a rainforest, the results based on the geometric graph have been shown to spuriously indicate a decrease in spatial biodiversity when no such trend was detected by the other types of neighbourhoods. We also show that the choice neighbourhood markedly impacts on the classification of species according to how strongly and in what way different species spatially structure species diversity. Clearly, in an analysis of spatial or local diversity an appropriate choice of local neighbourhood is crucial in particular in terms of the biological interpretation of the results. Due to its general definition, the approach discussed here offers the necessary flexibility that allows suitable and varying neighbourhood structures to be chosen.

Keywords biodiversity · exposure · neighbourhood · spatial · point pattern

Tuomas Rajala
Department of mathematics and statistics, University of Jyväskylä, Finland
E-mail: tuomas.rajala@jyu.fi

Janine Illian
School of Mathematics and Statistics, University of St Andrews, UK
E-mail: janine@mcs.st-and.ac.uk

1 Introduction

In view of an increasing threat to natural ecosystems and biological diversity world-wide, a fundamental question in ecology is whether depauperate systems function differently from or less efficiently than ecosystems and communities with higher diversity and, in the long run, whether loss of species with specific traits and functions will have an influence on productivity (Cardinale et al, 2000; Loreau et al, 2001). Clearly, in order to gain an understanding of and to monitor changes in biodiversity, appropriate measures of biodiversity have to be used (Magurran, 1988; Buckland et al, 2005). Hence, the construction of suitable measures of biodiversity has been the focus of much research in ecology. A large number of indices of diversity based on the relative abundance of a multitude of species have been discussed in the ecological literature, most notably the Shannon index and the Simpson index; several authors construct entire families of diversity indices (Hill, 1973; Tóthmérész, 1995). Most of these approaches either consider the total number of species, *species richness*, or the relative abundance of the species, *species evenness*, or both. These indices often differ in their relative emphasis on either of the two concepts. In addition, some indices focus more on the diversity among the rarer species whereas others emphasise the dominant species (Magurran, 2004).

To a different degree all these approaches concern the question as to how rich and how well balanced in species numbers the ecosystem is as a whole. In doing so, classical measures of biodiversity do not take the individuals' perception of (local) diversity into account but take on a "mean field" perspective on biodiversity. This is despite much ecological research in general having recently focused on an individual-based and hence spatially explicit understanding of population dynamics, in particular in the context of plant ecosystems (Law and Dieckmann, 2000; Hubbell et al, 2001). However, even though the idea of incorporating spatial information into the analysis of diversity is not new (Clark and Evans, 1954), only a few, scattered approaches exist in the literature. Within the ecological literature Wiegand et al (2007) introduce a spatial version of species richness, Podani and Czaran (1997) consider a measure of local compositional species presence-absence, and Shimatani (2001) defines a local version of the Simpson index. Reardon and O'Sullivan (2004) discuss a spatial Shannon index in a sociological context. Motz et al (2010) compare some measures of spatial and non-spatial diversity. However, as yet no general framework for defining spatial biodiversity exists. In this paper we introduce a flexible family of local biodiversity measures based on graphs associated with the spatial pattern formed by the individuals that generalises current approaches and provides this general framework.

More specifically, when analysing the diversity of a spatially mapped ecosystem, two different aspects of biodiversity may be distinguished; firstly, the diversity of an ecosystem as a whole in terms of the number of different species, the focus of classical (aspatial) biodiversity measures, and secondly the diversity of an ecosystem from the local perspective of an individual in terms of the spatial configuration of the individuals within and between species, i.e. "spatial biodiversity". Measures of spatial biodiversity describe the diversity in the immediate vicinity of each individual, i.e. in its local neighbourhood. Within the context of *spatial point process theory*, an important framework for statistical analysis and modelling of spatial point patterns, we use *graphs* as a flexible description of local proximity and hence an individual's "neighbourhood". We suggest measuring spatial biodiversity by flexibly defining the individuals' neighbourhood in a general way based on a variety of graphs and study how a change in the definition of the neighbourhood affects the performance of the resulting measures. By reflecting the neighbourhood structure in a graph we are able to both provide a unified framework which includes existing measures of local biodiversity

and to define a general family of measures by varying the definition of the neighbourhood as expressed by the graph.

This paper is organised as follows: the mathematical framework of spatial point processes and graphs is described in Section 2. Section 3 discusses different measures of spatial diversity and Sections 4 and 5 summarise results from a detailed simulation study and an application to an ecological dataset.

2 Spatial point patterns and characterisation of an individual's local neighbourhood

2.1 Point processes as models for point patterns

In this section we briefly summarise some basic notation; for further details on spatial point processes refer to Stoyan et al (1995), Møller and Waagepetersen (2003) and Illian et al (2008). A *spatial point process* is a random collection of points $X = \{x_i : i = 1, \ldots\}$ located randomly in $\mathbf{R}^d$. We assume that no duplicate points exist, and that the process is *stationary*, i.e. that the distribution of the shifted process $X_z = \{x_i - z : x_i \in X\}$ is the same for all $z \in \mathbf{R}^d$. Let $X(B) = card\{X \cap B\}$ be the number of points in some set $B \subseteq \mathbf{R}^d$ and $B(x,r)$ a r-ball centered at x. *Intensity* of a process X is the average number of points per unit area, $\lambda = \mathbf{E}X(B)$ with $|B| = 1$. Attaching a discrete mark (reflecting e.g. types or species) $t(x_i) \in \mathscr{S} = \{1, ..., S\}$ to each point of the process results in a *multitype* point process. Let $X_\tau = \{x_i \in X : t(x_i) = \tau\}$ denote the sub-process of points of type τ.

Complete spatial randomness (CSR) is modelled by a homogeneous spatial Poisson process with intensity parameter λ, where $X(B)$, the number of points in B, is Poisson distributed with parameter $\lambda|B|$ for any B, and the number of points $X(B_1)$ and $X(B_2)$ for any two non-overlapping sets B_1 and B_2 are independent random variables. If all the components of a multitype point process X are CSR processes, we call X multitype CSR.

In the following, we consider functions of the neighbourhood of a focal point x given that the focal point x belongs to the process X, using *Palm* measures $\mathbf{P}_x$ and expectations $\mathbf{E}_x$; under stationarity it suffices to condition on the origin o, in the following also referred to as a *typical point*. We assume that the stochasticity of the process can be accounted for by the Palm measures (Møller and Waagepetersen, 2003). We write $\mathbf{P}_{x,\tau}$ and $\mathbf{E}_{x,\tau}$ when we condition on $\{t(x) = \tau\}$. An example of this approach is *Ripley's K-function* (Ripley, 1977), a classical tool for analysing the scattering in stationary point patterns. It is defined as $\lambda K(r) = \mathbf{E}_o \sum_{x_i \in X \setminus \{o\}} \mathbf{1}(x_i \in B(o,r))$, i.e. the expected number of points within distance r from a typical point of the process. It can be used to detect clustering and regularity at varying spatial scales by comparing the estimated function of an empirical pattern to the function expected for CSR. In the following, we denote a restriction of the K-function to a subpattern X_τ of type τ by $K_{\tau\tau}(r)$.

2.2 Graph defined neighbourhoods

A *graph* G consists of a discrete set of *vertices* which are connected by *edges* (Marchette, 2004). We associate a graph $G(X)$ with the point process X by defining some edge relation which generates the edges. If an edge exists between x_i and x_j, we write $x_i \leftrightarrow x_j$ and say that x_i and x_j are *neighbours*. If the relation is not symmetric we emphasise this with the notation $\cdot \rightarrow \cdot$. The notation is also used in the sense "$x_i \leftrightarrow x_j$" $\Longleftrightarrow$ "$x_j \rightarrow x_j$ and $x_j \rightarrow x_i$". Finally, the *neighbourhood* of a point $x_i \in X$ is the set $ne(x_i) = \{x_j \in X : x_i \rightarrow x_j\}$.

We consider the following specific graphs but any other graph may also be used to define the neighbourhood of a point:

1. *Geometric graph with radius R*: For $R > 0$ and the Euclidian distance $d(x_i, x_j) \geq 0$, let

$$x_i \leftrightarrow x_j \Longleftrightarrow d(x_i, x_j) < R.$$

   This relation leads to the conventional definition of spatial proximity based on a fixed radius R. It may be generalised by considering a different R_τ for each type τ.
2. *k-nearest neighbours graph:* For $k > 0$, denote by $d_k(x_i)$ the distance from x_i to its kth nearest neighbour. Then the graph is given by the relation

$$x_i \rightarrow x_j \Longleftrightarrow d(x_i, x_j) \leq d_k(x_i).$$

   Unlike the geometric graph, the k-nearest neighbour graph focuses on the topology of the pattern rather than on linear proximity.
3. *Gabriel graph:* Let B_{x_i,x_j} be the open disc ($d = 2$) with x_i and x_j at the extremes of the diameter. Then the graph is given by

$$x_i \leftrightarrow x_j \Longleftrightarrow X(B_{x_i,x_j}) = 0.$$

   In other words, x_i and x_j are neighbours if the circular area between them is empty. This is a simple non-parametric description of proximity: two points are neighbours if they share a common space between them.
4. *Delaunay triangulation:* Assume that all triplets $x_i, x_j, x_k \in X$ are non-collinear and let $B(c,r)$ be the open disc with the border as the circumcircle of the triangle $\Delta(x_i x_j x_k)$. i.e. $d(c, x_i) = d(c, x_j) = d(c, x_k) = r$. Then we set

$$x_i \leftrightarrow x_j,\ x_i \leftrightarrow x_k,\ x_j \leftrightarrow x_k \Longleftrightarrow X(B(c,r)) = 0.$$

   This graph contains the same information as the well-known *Voronoi diagram* (Okabe et al, 2000). It is a triplet version of the Gabriel graph: points in a triplet are neighbours if they share enough empty space between them.

Figure 1 shows a realisation from a Poisson process with the four associated graphs. The neighbourhood of the focal point differs strongly depending on the definition. Unlike the geometric graph, the Gabriel and Delaunay graphs can connect points that are rather far apart as long as there is enough empty space between them. This might be of importance in practice. In applications where the local environment of individuals is of interest, the degree of "crowdedness" in different directions from an individual may provide a more realistic reflection of an "individuals's eye view" than, e.g., a neighbourhood based on a fixed radius. To illustrate this point further, the space around the focal point resulting from the different neighbourhood definitions is depicted in Figure 2. For the geometric graph the size of the neighbourhood space is fixed *a priori* and is the same for every point. For the other three graphs the space around the focal point depends on the local configuration of the pattern.

The geometric and the k-nearest neighbour graphs depend on the parameters R and k respectively, and we shall refer to them as *parameterized* graphs. By contrast, we use the term *nonparameterized* graphs for the Gabriel graph and the Delaunay triangulation as they do not depend on any parameters. Certainly, these graphs may be further generalised, for example by considering the second order Delaunay graph where the neighbours defined by a (first order) Delaunay neighbours are also neighbours. In this paper we focus on the graphs given above; for further information on spatial graphs see Marchette (2004).

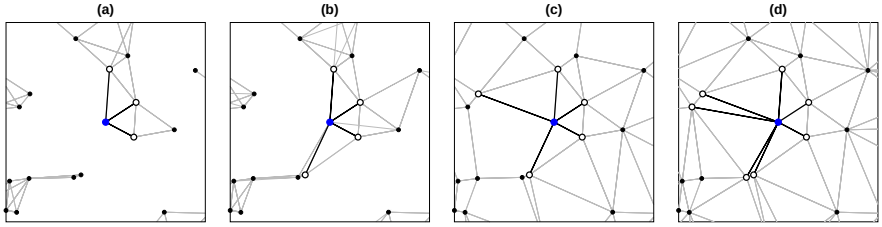

Fig. 1 Simulated spatial pattern with four associated graphs, the geometric graph (a), the 4 nearest neighbour graph (b), the Gabriel graph (c) and the Delaunay triangulation (d). Neighbour connections for different types of graphs of the focal point in the middle are highlighted by thick lines, and neighbours by circles.

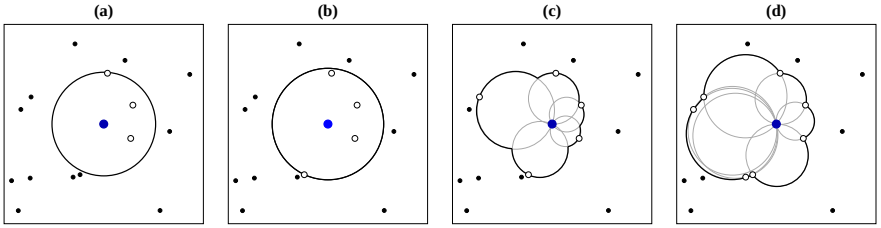

Fig. 2 The neighbourhood space of the point in the middle. Pattern and graphs as in Figure 1.

2.3 Diversity: frequencies of types and spatial mixing of types

As mentioned above, we distinguish between *aspatial* and *spatial* diversity. Defining and measuring aspatial diversity has been central to the biodiversity discussion in ecology (Buckland et al, 2005) and a large number of measures based on species counts have been considered (Magurran, 2004). Spatial aspects of diversity have been included into the studies by considering the increase in the number of species with increasing sampling area, i.e. in terms of *species-area-relation* curves (see e.g. Scheiner, 2003; McGill et al, 2007). This approach differs from the approach taken here as it measures the number of species per area, irrespective of the individuals' location or their neighbourhood composition.

Two aspects of spatial diversity, termed *scattering* and *exposure*, may be distinguished. Spatial scattering describes how a specific type τ is arranged within the observation window. The points may be *clustered*, i.e. show an aggregated pattern, or exhibit *regular* scattering, or be randomly and independently scattered (CSR). Since the theory and statistics of spatial scattering have been studied extensively in the literature (Møller and Waagepetersen, 2007; Illian et al, 2008), we focus on exposure here. Spatial exposure describes the neighbourhood structure of a typical individual of one type in terms of the other types. An individual has a high degree of exposure or *mingling* if its neighbourhood is highly diverse, i.e. if many neighbours from other types are located in its vicinity. The opposite situation of a largely conspecific neighbourhood is referred to as *segregation*. A pattern with high small scale spatial diversity is strongly mingled. If, instead, the pattern shows high segregation, it can be split into homogeneous patches with little or no overlap and low diversity within these patches.

Figure 3 illustrates the two aspects, scattering and exposure, in a small example with artificial data. Here, varying levels of scattering, ranging from clustering to regularity are illustrated on the horizontal axis and varying degrees of exposure, ranging from segregation to mingling on the vertical axis. Clearly, exposure and scattering are not independent. In particular, the bottom plot of the middle column shows that a strong segregation effect can

force the points into clustered patterns even though the individual patterns have not been generated by clustering mechanisms.

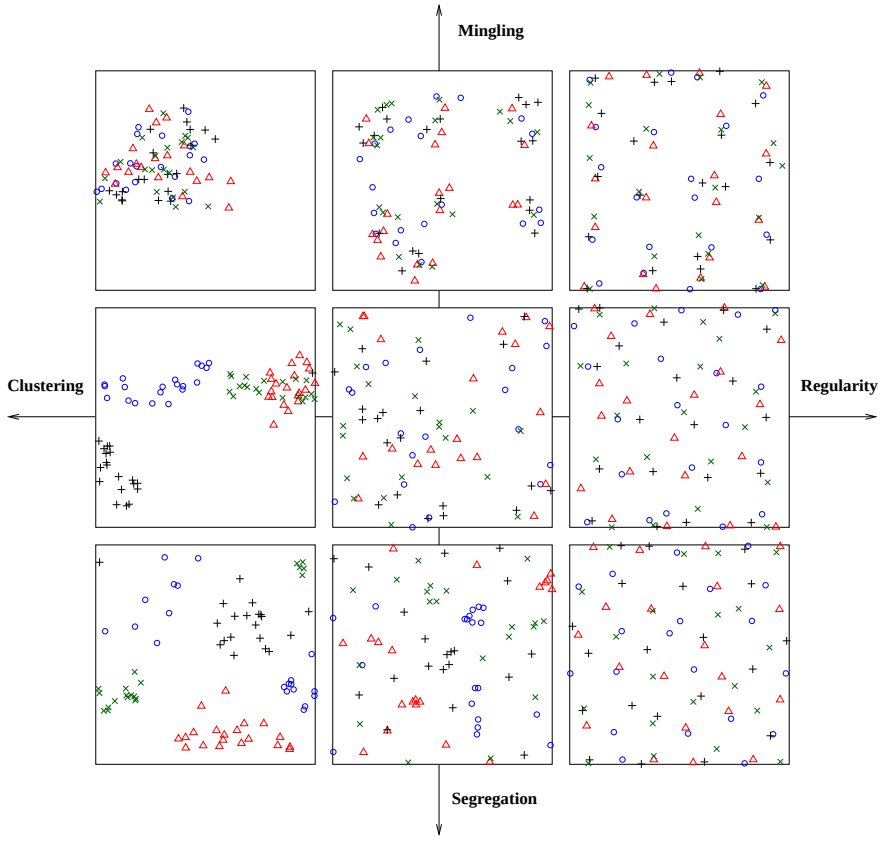

Fig. 3 Illustration of the two aspects of spatial diversity, scattering and exposure. All nine plots have the same aspatial diversity, but the spatial diversity varies. The horizontal axis shows varying levels of scattering, ranging from clustering to regularity. The vertical axis shows varying degrees of exposure, ranging from segregation to mingling. The central plot shows complete spatial randomness. Based on similar figures in e.g. Pielou (1977) and Shimatani and Kubota (2004).

3 Measuring spatial exposure

We will now discuss how different approaches to determining the diversity in an individuals' neighbourhood (Podani and Czaran, 1997; Aguirre et al, 2003; Shimatani and Kubota, 2004; Illian et al, 2008), may be used to assess spatial exposure, and present these within the framework of spatial point processes coupled with graphs to yield a family of measures of spatial biodiversity.

3.1 Local abundance

For notational purposes consider any graph, e.g. one of those given in Section 2.2. For an individual $x_i \in X$ and a type $\tau \in \mathscr{S} = \{1, \ldots, S\}$, we define

$$\begin{aligned}
\delta(x_i) &:= \sum_{x_j \in X \setminus \{x_i\}} \mathbf{1}(x_i \to x_j), \\
\delta_\tau(x_i) &:= \sum_{x_j \in X \setminus \{x_i\}} \mathbf{1}(x_i \to x_j,\, t(x_j) = \tau), \\
\delta_=(x_i) &:= \sum_{x_j \in X \setminus \{x_i\}} \mathbf{1}(x_i \to x_j,\, t(x_j) = t(x_i)), \\
\delta_{-\tau}(x_i) &:= \delta(x_i) - \delta_\tau(x_i), \\
\delta_\neq(x_i) &:= \delta(x_i) - \delta_=(x_i).
\end{aligned}$$

Apart from the first one, these local abundances are conditional: the abundance of neighbours of type τ, of neighbours that have the same type x_i-, of neighbours that are not of τ and of neighbours that are not of the same type as x_i. Under the stationarity assumption, we can write for a typical point $o \in X$ and types $\tau, \gamma \in \mathscr{S}$

$$\overline{\delta} = \overline{\delta}_{\mathscr{S}} := \mathbf{E}_o \delta(o), \qquad \overline{\delta}_\star := \mathbf{E}_o \delta_\star(o), \qquad \overline{\delta}_{\gamma,\star} := \mathbf{E}_{o,\gamma}(\delta_\star(o)),$$

where $\star$ is one of the symbols $\{=, \neq, \tau, -\tau, \mathscr{S}\}$. The mean local abundances describe the expected neighbourhood composition in the pattern, either irrespective of types ($\overline{\delta}$) or referring to specific types ($\overline{\delta}_\star$). The conditional mean $\overline{\delta}_{\gamma,\star}$ is useful when we are only interested in the neighbourhood of individuals of type γ.

We also consider the proportional abundances

$$\pi_\star := \frac{\overline{\delta}_\star}{\overline{\delta}}, \qquad \pi_{\gamma,\star} := \frac{\overline{\delta}_{\gamma,\star}}{\overline{\delta}_{\gamma,\mathscr{S}}} \qquad \text{and} \qquad p_\star := \frac{\lambda_\star}{\lambda}$$

setting $0 := \frac{0}{0}$ when necessary. Here π_τ denotes the mean proportion of τ neighbours amongst all neighbours of o. The summary $\pi_{\gamma,\star}$ is conditional on $\{t(o) = \gamma\}$. If π_τ is interpreted as a local quantity, then p_τ is its global counterpart. Note that aspatial diversity indices only use the information contained in p_τ.

3.2 Exposure summaries

With the above notation, an index of spatial exposure with a neighbourhood based on a parameterized graph may be written as a function of the parameter. This provides us with a powerful and flexible tool as we can consider the value of the index, and hence the biodiversity, at different spatial scales rather than as a single value summarising spatial diversity at several spatial scales (Illian et al, 2008). If, however, an index is preferred (for reasons of cost, convenience, computation time or simplicity), the notation allows the use of nonparameterized neighbourhoods in a straightforward way.

Pielou (1961), Dixon (1994) and Ceyhan (2009) consider asymptotic tests of segregation based on contingency tables and on $\overline{\delta}_{\tau,\neq}$ for the special case of $S = 2$ and the 1-nearest neighbour graph. At the cost of theoretical convenience, we assume no such restrictions and now consider different measures of local diversity. The (aspatial) *Simpson index* of biodiversity is defined as $\alpha_0 = 1 - \sum_{\tau=1}^{S} p_\tau^2$. It measures the deviation from uniformity of abundance

indicating, for example that some species with relatively high abundance dominate the population, with a high value of α (Magurran, 2004). Shimatani (2001) defines a local index based on Ripley's K-function, and defines the *spatial Simpson index* for $r > 0$ as

$$\alpha(r) = 1 - \sum_{\tau=1}^{S} \frac{\lambda_\tau^2 K_{\tau\tau}(r)}{\lambda^2 K(r)}.$$

Since, by definition $\overline{\delta} = \lambda K(r)$ when a neighbourhood defined by the geometric graph is used, we can replace r by θ and hence generalise the index as

$$\alpha(\theta) := 1 - \sum_{\tau=1}^{S} p_\tau \frac{\overline{\delta}_{\tau,\tau}}{\overline{\delta}}.$$

This can then be calculated for different neighbourhoods, with the parameter θ controlling the underlying graph the neighbourhood is based on. Note that the spatial Simpson index, like the aspatial index, operates on the population level, as a summary across all species. The interpretation is analogous; if we randomly pick one point of the pattern as a focal point, and another point from the focal point's neighbourhood, the index describes the probability that the two are from different species.

Wiegand et al (2007) introduce a spatial version of species richness, the *individual species area relationship (ISAR)*. We again generalise this based on different types of neighbourhoods and define

$$\beta_\tau(\theta) := \sum_{\gamma=1}^{S} \mathbf{P}_{o,\tau}(\, \delta_\gamma(o) > 0). \tag{1}$$

This measures the number of species in the average neighbourhood of an individual of species τ. We can consider $\bar{\beta}(\theta) = \mathbf{E}_\tau \beta_\tau(\theta)$ to yield an index for the whole population similar to the spatial Simpson index. An average population level measure has been discussed by Shimatani and Kubota (2004), but we focus on the species level version in equation (1) as it provides more detailed information.

The *mingling index* also operates at the species level. It is defined as the fraction of neighbours of a different species among the neighbours of a point of species τ, i.e.

$$M_\tau(\theta) := \frac{\overline{\delta}_{\tau,\neq}}{\overline{\delta}_{\tau,\neq} + \overline{\delta}_{\tau,=}} = \pi_{\tau,\neq}.$$

For practical reasons this index was restricted to the 4-nearest neighbours graph in its original formulation (Lewandowski and Pommerening, 1997) and not generalised to other values of k. The general definition for $\theta = k > 4$, however, might be more interesting in the context of data sets with larger numbers of species. Wiegand et al (2007) consider $1 - M_\tau(\theta)$ and call it the local dominance of species τ. Note that if species abundances are equal for all species in a data set, the mean mingling index across species equals the spatial Simpson index.

The entropy based Shannon index may also be generalised to a spatial Shannon index (Reardon and O'Sullivan, 2004), but the very low abundances of rare species within the individuals' neighbourhoods lead to numerical problems in the estimation (Magurran, 2004), especially when global species richness is high and neighbourhoods are small. Podani and Czaran (1997) discuss an alternative way of using Shannon information by comparing the observed and expected CSR abundance vectors by the log-likelihood-ratio for a binomial model.

Bossdorf et al (2000) note that the interpretation is rather complex. Since we aim to illustrate and assess the effect of varying the definition of the neighbourhood of an individual, we focus on measures with simple interpretations when $S >> 2$: the spatial Simpson index, the mingling index and ISAR.

3.3 Estimation and edge correction methods

The indices can be estimated by replacing the component expectations with the appropriate sample means. It is important to acknowledge the bias introduced by *edge effects*, which affect the estimation of quantities for points near the edge of the observation window. If the structure of the pattern outside the window is unknown, bias is introduced (Baddeley, 1998). For instance, in the context of the geometric graph with parameter r, the number of neighbours for a point less than a distance r away from the edge is likely to be too low.

Several approaches to correcting this bias have been discussed in the literature (see e.g. reviews in Illian et al (2008) and Møller and Waagepetersen (2003)). These correction methods have been derived for stochastic geometry based on the geometric graph, and hence it is not clear that they are also appropriate when different types of graphs are been used. The *translation correction* is suitable under stationarity and when a measure is based on counts of pairs of points. It may be used to estimate $\overline{\delta}, \overline{\delta}_\star$ and $\overline{\delta}_{\gamma,\star}$ in the Simpson and the mingling index, yielding ratio-unbiased estimators. However, the summaries are of ratio form where the border effect affects both the numerator and the denominator in a similar way, and hence the bias is likely to cancel out, as discussed in Illian et al (2008), p. 193. We have verified this to be true with a simulation experiment (results not shown).

The ISAR index is related to nearest neighbour summary characteristics where a common methods for edge effect reduction is to use some form of *minus sampling*. Most elaborate approaches use a correction that varies for each point, such as the Hanisch estimator where a point is excluded if its nearest neighbour distance is greater than the distance to the border. These minus sampling strategies are based on results derived for the geometric neighbourhood relation. We use the simplest form of minus sampling here where the contributions to a summary from all points that are inside a fixed buffer zone from the border are disregarded. This method reduces the bias well but has the disadvantage of leading to a loss of data. For the estimation of the sample means we consider only the contribution of those points for which the whole neighbourhood is inside the observation window. With the geometric graph and $r \in [0, r_{max}]$, minus sampling discards points less than a distance r_{max} from the edge. For k-nearest neighbours the minus range is estimated using the CSR approximation $k_{max} < (\lambda \pi r_{max}^2)$. We use this estimated minus range also for the nonparameterized neighbourhoods.

4 Simulation study

In order to assess the performance of the different indices as well as the effect of the choice of neighbourhood on the performance we run a simulation study based on synthetic data. Informed by this simulation study, we then assess the performance of the measures in practice and apply the indices to data from a tropical rainforest to analyse the change of local diversity over time and to analyse the magnitude of exposure of different species. [...]

4.1 Simulated patterns of varying species richness and evenness

Since spatial scattering and exposure are not independent we vary both aspects of spatial diversity in this simulation study. We consider nine main classes of point patterns simulated in a window $W = [0,1]^2$. The classes comprise three categories reflecting three levels of intra-species scattering: clustered, no scattering effect and regular. In addition, three levels of inter-species exposure are considered: mingled, no exposure effect and segregated. Within each of the nine classes the strength of the exposure and scattering effect are equal for all types. We simulate each class 100 times using the algorithm described in Appendix B; the patterns in Figure 3 were also generated with this algorithm. For each simulation, the three diversity summaries $\alpha(\theta), \beta_\tau(\theta)$ and $M_\tau(\theta)$ are calculated using neighbourhoods based on the Gabriel, Delaunay, geometric and k-nearest neighbours graphs. We then compute the mean mingling index and the mean ISAR over species so that we can compare them to the spatial Simpson index.

Furthermore, we repeat the above procedure for two types of abundance vectors, each with varying species richness, first for a vector with $S = 4$ and $n = 40$, from now on referred to as 'low richness', and for a vector with $S = 30$ and $n \approx 300$, referred to as 'medium richness'. For both types of abundance vectors three different levels of evenness are considered, ranging from complete evenness, via medium evenness, to dominance. This yields 6 different abundance vectors (Table C.1).

In summary, we conduct a series of simulation experiments to assess the ability of the summary characteristics to distinguish among patterns exhibiting different degrees of exposure. In each of the different experiments we vary the richness of the pattern, the evenness of abundances, the degree of clustering of species and the definition of the neighbourhood. In the following, the different richness-evenness-clustering-neighbourhood combinations are referred to as 'RECN combinations'.

4.2 Nonparameterized neighbourhoods

4.2.1 Low species richness

We first consider the Gabriel and the Delaunay graph. For each RECN combination, we simulate the pattern 100 times. From the simulations we compute each summary index to obtain three empirical distributions corresponding to the three exposure levels. We then compare these distributions using Mann-Whitney's signed rank test. As higher exposure levels should be reflected in higher index values, we use a one-sided test to test if the summary values for segregated patterns are lower than in the no exposure effect case, and if the values for mingled patterns are higher than in both the segregated and no exposure effect case. The results from the significance tests for the low richness vectors are shown in Table C.2.

We initially focus on the effect of the different degrees of scattering on the performance of the summary characteristics. For *clustered* patterns all indices distinguish well between the different levels of segregation, with both neighbourhoods. Only in the case of the very uneven vector, the spatial Simpson index with the Gabriel neighbourhood fails to separate segregated patterns from those with no exposure effect. In the same situation, the mingling index performs well. Recalling that the mean mingling index equals the spatial Simpson index for complete evenness this indicates that in uneven patterns the power of the spatial Simpson index is reduced when the number of neighbours is low.

For patterns with *no scattering effect* the mean mingling index and the spatial Simpson index both perform well. However, the ISAR with the Gabriel neighbourhood fails to distinguish between the different exposure levels and only one of three tests is significant in each evenness class. The results with the Delaunay graph are better, indicating that ISAR requires larger numbers of neighbours to perform well since it is a purely cumulative summary. The ratio based mingling and Simpson work well even with the smaller number of neighbouring points in the Gabriel graph.

Regular patterns are problematic for all summaries statistics. This is because these patterns consist of S superimposed regular patterns, and hence irrespective of the exposure level, the probability that non-conspecifics are found between two conspecific points is high everywhere. This demonstrates once again that scattering and exposure are not independent.

A comparison of the performance across the different levels of evenness reveals that understanding the effect of evenness is not straightforward. The summary characteristics perform best for patterns with medium unevenness, and worst for patterns with strong unevenness. Some of this effect may be due to the minus-sampling scheme. In a small simulation study (results not shown) with a smaller minus-sampling radius indicated that the power improves for medium and dominated vectors, especially for the ISAR, even though the reduced radius clearly introduces bias. This might have been caused by the many rare species in the data as some of these might be only present in the border buffer zone, and hence not contributing to the exposure estimation leading to an increased variance of the mean summary characteristic. The mingling index is apparently more robust to this effect.

4.2.2 Medium species richness

Table C.3 summarises the results for medium richness. The mean mingling and spatial Simpson indices now perform well due to the larger sample size, and even for regular patterns all tests are significant. However, ISAR still does not distinguish the different levels of exposure as the number of points in the neighbourhoods is apparently still too small for the cumulative summary characteristic to perform well. ISAR in combination with the Delaunay graph performs well for medium and high evenness. However, as before, due the small abundances for some rare species in the patterns with low evenness, edge correction removes some of these species and thus directly affects the mean ISAR.

The results in table C.3 also again emphasise that the effects of scattering and exposure are not independent as all indices perform worse for regular than for clustered patterns. In addition, simulated patterns with a strong exposure effect result in clustered patterns even in the absence of an explicit spatial clustering mechanism (recall the bottom plot in the middle column in Figure 3 for an example).

In conclusion, measures of spatial exposure based on both nonparameterized neighbourhoods perform well to a certain extend. Measures based on the Delaunay neighbourhood perform better (with 134 out of 162 significant tests indicating that patterns can distinguished correctly) than the Gabriel neighbourhood (with 122 out of 162 significance tests), a difference which can be explained by the smaller average neighbourhood size of 4 for the Gabriel compared to 6 for the Delaunay graph (as calculated for the case of CSR). The Delaunay neighbourhood should clearly be preferred in applications, especially in the context of non-clustered patterns. For the mean ISAR to perform well more individuals have to be included in the neighbourhood of a individual than for the mean mingling or the spatial Simpson index. The latter two perform quite well with both neighbourhoods when exposure effects

in non-regular patterns are assessed, and performance improves with increasing sample size and richness.

4.3 Parameterized neighbourhoods

We now compare measures of exposure based on the geometric and the k-nearest neighbours graphs. The parameters used in the calculation were $\{r = 0.01, 0.02, ..., 0.3\}$ for the geometric graph, and $\{k = 1, 2, ..., 15\}$ for small and $\{k = 1, 2, 4, ..., 80\}$ for medium evenness in the k-nearest neighbour graph, adjusting for the increased intensity. For each RECN combination, 100 segregated and mingled cases were simulated, each producing a summary function trajectory over each parameter range. These trajectories were then checked as to whether or not they remain completely inside a 95%-trajectory-envelope obtained from 100 simulations with no segregation effect. This testing procedure is known as an *envelope test* (Illian et al, 2008, p. 455). Here the segregated and mingled patterns are considered as individual data. We modified the test to be only one-sided, so that a segregated trajectory should be completely below, and a mingled trajectory above, the 95%-envelope.

4.3.1 Low species richness

Table C.4 gives the fraction of significant envelope tests for each of the low richness vectors. The most striking result is that for clustered and segregated patterns, all summary characteristics show a very low power when the k-nearest neighbour graph is used. The performance is slightly better with the geometric graph, where the power is decreasing with increasing unevenness. Why do all summary characteristics in combination with the k-nearest neighbour graph perform so poorly? In the absence of inter-species interaction the locations of conspecific clusters are not constrained. Hence individuals from one species appear in the neighbourhood of other species with a probability that is proportional to cluster diameter and window area. In our simulation the mean cluster diameter is small compared to the window area, such that clusters rarely overlap and hence patterns typically appear segregated. This then leads to wide summary envelopes. Also, in some cases, two smaller conspecific clusters form two rather than one big cluster, which increases the probability that one of the k-nearest neighbours is in a non-conspecific cluster. This is because the number of neighbours deterministically increases by one with each increase in the parameter with the nearest neighbour graph, whereas with the geometric graph the number of neighbours increases stochastically with increasing parameter.

With both types of neighbourhood the characteristics distinguish mingled and clustered patterns from non-mingled patterns with 100% power. However, the performance of the mean mingling index and the spatial Simpson deteriorates for patterns with no scattering effect and regular patterns whereas ISAR performs well. This might be due to the cumulative and hence more stable nature of ISAR, resulting in narrower envelopes. The power of the mingling and the spatial Simpson index improves with increasing unevenness.

4.3.2 Medium species richness

For patterns based on the medium richness vectors (Table C.5) almost all tests are significant, i.e. a larger sample size definitely improves the power of the summary characteristics to distinguish pattern with different levels of exposure when several spatial scales are analysed simultaneously.

Overall, the characteristics based on parametrized graphs work similarly well. In some cases those based on the geometric graph perform better in other cases those based on the nearest neighbour. The only exception to this occurs for segregated and clustered patterns. Here the characteristics using the geometric graph versions have problems, whereas nearest neighbour versions fail completely. All this is related to a small sample size, and if we have a larger sample, all summaries with both neighbourhoods are suitable for studying exposure effects.

4.4 Conclusions from the simulation study

Based on the simulation study we may conclude that the choice of the nonparameterized neighbourhood has an effect on the performance of the measures of exposure, albeit a small one, and that it depends on the choice of summary characteristics. Both the mingling and the spatial Simpson index work similarly well when they are based on the Gabriel and the Delaunay graph, but these non-parameterized neighbourhoods are too small for ISAR to perform well even with larger patterns.

Of the parameterized neighbourhoods, the k-nearest neighbours graph does not work as well as the geometric neighbourhood in a small sample of clustered patterns. Otherwise the different neighbourhoods perform similarly well. The choice of summary characteristic seem much more important here, as ISAR clearly outperforms the mean mingling and the spatial Simpson index.

In conclusion, the summary characteristics based on all the graphs but the Gabriel graph distinguish well between the exposure levels of the simulated patterns. With the exception of clustered patterns in small samples, the k-nearest neighbours version is a suitable alternative to geometric neighbourhood when parameterized neighbourhoods are of interest.

5 Applications

5.1 Rainforest trees in the Barro Colorado Island plot

In order to assess the performance of the measures in the context of real data, we estimate the different spatial diversity indices in an ecological data set and study how (spatial) diversity changes over time. The data have been derived from a long term rainforest study plot on Barro Colorado Island (BCI) in Panama (Condit, 1998; Hubbell et al, 1999, 2005). In a plot of size 500m$\times$1000m every tree with stem diameter at breast hight larger than 1cm was recorded, along with the spatial coordinates, species and diameter at breast height. Data collection has been repeated six times in the years 1981, 1985, 1990, 1995, 2000 and 2005, amounting to roughly $2 \cdot 10^5$ data points and 300 species each year. The data have been analysed before with approaches that use methods based on the geometric graph, e.g. in Condit et al (2000); McGill et al (2007); Wiegand et al (2007); Morlon et al (2008); Waagepetersen and Guan (2009). We focus here on a simplified analysis of the data rather than on a detailed analysis of the entire data set, and point out the impact of varying the neighbourhood definition on the results.

5.2 Development of local diversity during the years 1981-2005

We calculate the exposure indices for each year using neighbourhoods based on the Gabriel, the Delaunay, the k-nearest neighbours and geometric graph, and fix the parameters $k = 7$ and $R = 1.95$ meters to be close to the expected nonparameterized neighbourhood sizes. The indices are estimated using all alive trees with dbh$>$10cm as focal points, and we consider only those species which have at least 30 individuals with dbh$\geq$10cm in each census. Thus we estimate the local diversity of 92 species, roughly 10% of the measured plants. However, all measured and alive plants contribute to the indices, as individuals of any size and species are considered as neighbours of focal points. In other words, we focus on the local diversity of well established plants in the forest.

We compare different years with Mann-Whitney tests to check if spatial diversity is increasing or decreasing. Tests are paired by species. For comparison, we also calculate the aspatial Simpson index for each year, which results in a u-shaped rather than a monotone trend over time, with a minimum value for year 1985 (see Appendix C Table C.6).

Table C.7 summarises the change of values of mingling index and ISAR using the four neighbourhoods. The mingling index values increase from 1985 to 1990 with all neighbourhoods; those with the geometric have a stronger significance than others. A significant change in the values could not be detected for the other years, which is probably due to the small neighbourhood size of about 6 neighbours relative to the total number of species. The values of the ISAR change more markedly. With the geometric neighbourhood, the values increase consecutively between 1981, 1985 and 1990, then decrease from 1990 to 1995 and further to 2000 and 2005. The values based on Delaunay and k-nearest neighbour neighbourhoods indicate only a decrease between 1981 and 1985, with an additional decrease between 1995 and 2000 with k-nearest neighbours graph.

For the 6 most abundant species (Table C.8, see also Figure C.1) the values for the mingling index increase between 1985 and 1990 with all neighbourhoods, indicating a small decrease in the local dominance of these species. The increase in local richness between 1985 and 1990 is also found with ISAR combined with the geometric neighbourhood, but the sequential decrease between 1990 and 2005 is less clear.

If only the results based on the geometric graph were considered - as is commonly done - one would conclude that the diversity in local neighbourhoods of individual plants in the BCI plot have first increased and then decreased over the years. However, the geometric graph also captures scattering effects, resulting in biased exposure measurements. One way of avoiding this is by scaling the neighbourhood relative to the local intensity as the adaptive neighbourhoods of k-nearest neighbour, Gabriel and Delaunay graph do (see also the weighting scheme in Morlon et al, 2008). Then not only is the hypothesis for the consecutive change of local species diversity rejected, but we also observe opposite results to those obtained with the geometric neighbourhood. Effects such as overall thinning should be captured in the analysis of point scattering in relation to the area, not in the analysis of individual species' neighbourhood in relation to other species. Therefore, when analysing the pattern formed by a biological community one should also consider sophisticated neighbourhoods rather than only the geometric graph provides, to account for the changes in scattering effects that may lead to spurious changes in measures of exposure.

5.3 Change in spatial Simpson index values

In this example we consider the spatial Simpson index for BCI in each census year using the two parameterised neighbourhoods and plot it as a function of the relevant parameter. This is done in order to see how the overall spatial diversity across species is affected by the neighbourhood definition. As in the previous example we focus on the neighbourhoods of plants with dbh>10cm of species with abundance over 30, while smaller and/or rarer plants still contribute to the neighbourhoods.

Figure 4 shows the differences in the spatial Simpson index for each year y compared to the year 1981 calculated as $\alpha^{y}(\theta) - \alpha^{1981}(\theta)$. If the value is higher than 0 at a neighbourhood size θ spatial diversity in the corresponding year is higher than in 1981 at that particular scale. The results for the geometric graph have been plotted in area units πr^2 so that the similarity to the measure based on the nearest neighbour graph becomes clearer.

The local diversity, measured in the neighbourhood of established plants and reflecting an overall lack of dominance, has declined slightly over the years. The strongest declines happened between 1990 and 1995 with diversity dropping by approx. 0.2%. The decline over the entire period between 1981 and 2005 amounts to approx. 0.8%. Expressed as an odds ratio this means that if an average tree is chosen at random from the neighbourhood of a focal species the change is 1.3 times higher in 2005, than in 1981 that it is of the same species. Variances of the estimates have not been addressed in here.

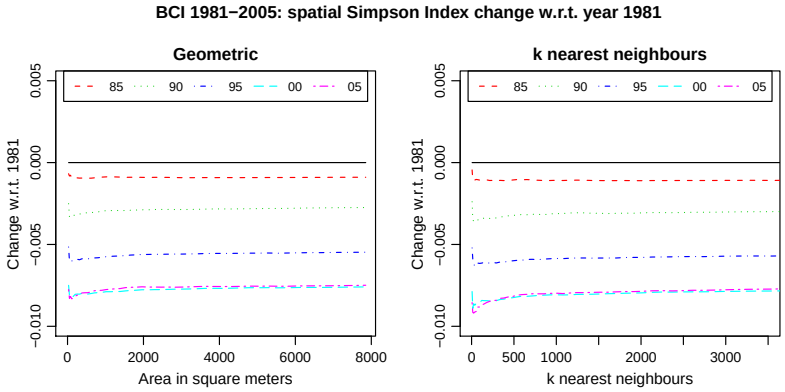

Fig. 4 Spatial Simpson index of BCI years 1981-2005. Computed from trees with diameter over 10cm and species abundance atleast 30.

In this example, different neighbourhoods lead to almost identical results. Averaging over different species apparently smoothens out the local scale variations of clustering each species internally exhibits, possibly as a function of the inhomogeneous environment. However, if a similar analysis is done which does not average across species, but classify the species according to different measures of spatial exposure these effects become visible as is clear in the following example.

5.4 Classifying species based on their local richness

In this section we aim to characterise an ecological community by identifying different classes of species with different types of spatial exposures. A similar classification of tree species has been done for the 1995 BCI census in Wiegand et al (2007). We re-analyse the same data but base the analysis on several types of neighbourhoods rather than on the geometric neighbourhood alone. Following the approach therein, each species is classified as either a diversity repeller, as neutral or as an accumulator at all relevant spatial scales, i.e. for all neighbourhood sizes. The classification is based on an envelope test against an inhomogeneous Poisson model, repeated separately for each species. Inhomogeneity in the null-model is assumed to account for all environmental factors such as slope and soil composition, which vary continuously in space with covariation ranges larger than 50m. Again following Wiegand et al (2007) the analysis concentrates on all species with at least 70 individuals of dbh$\geq$10cm, yielding a total of 63 focal species. All trees with dbh$\geq$10cm were used as potential neighbours of the focal species.

At each spatial scale of the neighbourhood, a species is classified as a diversity accumulator if its ISAR value is higher than the 97th highest value of the 100 values simulated from the null-model. So, an accumulator is defined as a species surrounded by more species than would be expected if it was randomly scattered. Similarly, a species is classified as a diversity repeller if its ISAR value is lower than the 3rd lowest simulation value, so it has fewer than the expected number of species in its vicinity. Species whose ISAR values remain inside the envelopes are termed diversity neutral.

Figure 5 summarises the results, again in area units to facilitate comparison. With the geometric neighbourhood more than 50% of the 63 species are classified as repellers at ranges $<$10m, or areas $<$300m^2. Only a small proportion of the species, less than 10%, are accumulators, and they are mainly detected at ranges 10-30m (300-2800m^2).

The k-nearest neighbours graph results are markedly different. Less than 20% of the species are classified as repellers when the neighbhourhoods consist of less than 50 nearest trees. At the same scale, more than 10% of the species are classified as diversity accumulators. Furthermore, many of the species identified as repellers with the geometric neighbourhood are classified as neutral or even as accumulators at the corresponding neighbour count. For example for $r = 10$m and CSR expected neighbour count in such size disc, $k = 17$, 6 species are classified as repellers with both neighbourhoods. However, 17 species classified as repellers with the geometric graph appear neutral using the k-nearest neighbour graph, and one species is classified as a repeller with the geometric graph and as an accumulator with the nearest neighbour version.

We repeat the classification of species into repellers and accumulators for each BCI census year using four fixed neighbourhoods. The issues caused by minus sampling are not as pronounced here as they are in Example 4.3 due to the large number of data points. Figure C.2 shows that the measures based on the Gabriel and Delaunay graphs yield results very unlike the parameterised graphs, classifying half of the species as accumulators, and nearly none as repellers. With these small neighbourhoods that are expanding always in the direction of empty space and do necessarily remain not inside clusters, a randomly shifted individual has a higher probability to have different species around it than in its original location, which tends to be within a cluster formed by individuals from the same species. Many of the species that are classified as repellers with the geometric graph are in fact found to be accumulators with the non-parameterized neighbourhoods. There is one common feature in these partly contradictory results. The neighbourhood scale at which both repellers and accumulators can no longer be distinguished is similar for both parameterized neighbour-

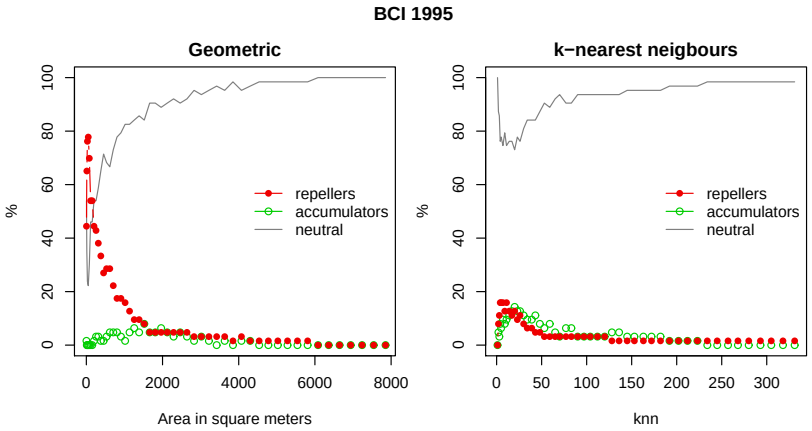

Fig. 5 Diversity accumulators and repellers in BCI 1995 census. Percentage of the 63 focal species.

hoods, roughly 35m (4000m^2) which with the average intensity of 0.045 trees/m^2 amounts to about 170 neighbours.

These results indicate that the choice of neighbourhood has a strong influence on the outcome of the classification of the species clearly and critically impacting on the biological interpretation of the results.

6 Discussion

More and more fully mapped data sets of biodiverse ecological communities have become available and hence there has been an increasing interest in individual-based modelling as well as in the spatially explicit analysis, based on spatial point process theory, of these ecosystems. In particular, the biodiversity and complexity of rainforests has been studied intensively in order to understand the mechanisms that sustain them. In this paper we have focused on the notion of spatial (or local) biodiversity taking on the plant's eye view with regard to biodiversity (Mahdi and Law, 1987; Law et al, 2009).

Classically, the analysis of spatial point pattern data considers functions of distance measures which imply the notion of a neighbourhood, i.e. the local vicinity of the individual points. Here we generalise the definition of the neighbourhood based on graphs to provide, for the first time, a general framework for the definition of measures of spatial biodiversity and study the effect of varying the neighbourhood on the performance of the measures of spatial biodiversity. We focus on measures of spatial exposure, an aspect of diversity related to the local mixing of different types of individuals in space.

The study reveals that the most commonly used neighbourhood, the geometric neighbourhood, is sensitive to the spatial arrangement of the points in relation to the study area, not just in relation to the points themselves, i.e. measures based on it do not distinguish well between scattering and exposure. This problem is much less pronounced when other neighbourhoods, defined by the (nonparameterized) Gabriel or Delaunay graphs or the (parameterized) k-nearest neighbours neighbourhood, are used. The latter three neighbourhoods separate the mixing of the different types without being affected by scattering effects, i.e. the spatial behaviour of the individual types. In an analysis of the spatial diversity in a rainforest,

the results based on the geometric graph are shown to disagree with those based on the other neighbourhoods, indicating a decreasing biodiversity while no clear trend was detected by the other types of neighbourhoods.

One might think of the neighbourhood defined by the k-nearest neighbour graph as the neighbourhood resulting from a locally weighted geometric graph where higher local abundance is weighted such that the radius become smaller. The discrepancy of the results is therefore connected to the variation of neighbourhood counts: A randomly dislocated individual of a geometrically repelling species is likely to have a different amount of neighbours than it has on its original location. This directly affects the detected species richness: on average, more neighbours amount to more species. This means that the scattering effect, which is due to environmental variation and intraspecific dispersal mechanisms, and the exposure effect, what the ISAR is ultimately trying to estimate, are very difficult to disentangle when the pattern is inhomogeneous.

In conclusion, the neighbourhood type is an important factor in the analysis of spatially explicit data and it affects our understanding of the spatial behaviour in a dataset. It is crucial to decide which neighbourhood relation best describes the spatial structures in the dataset, in relation to those aspects of spatial diversity (or other spatial behaviour) that are of interest in a specific study. Our results show that in the context of spatial diversity as reflected in scattering and exposure the (classical) geometric neighbourhood is not the only option for testing and answering the globally important ecological questions and that it might yield misleading results. This has important consequences on the biological interpretation of the results, e.g. with regard to theories of biodiversity as done in Wiegand et al (2007). Analyses based on neighbourhoods other than those defined by the geometric graph will identify fewer species as spatially structuring species diversity than the results in Wiegand et al (2007) and are also likely to contradict that analysis as to the nature of the spatial structuring. It is the flexibility of the approach taken here that allows suitable and varying neighbourhood structures to be chosen. It offers the possibility to carefully define further measures of spatial biodiversity that may be adapted to a specific situation as well as the relevant research question.

Clearly, the approach here may be generalised in many ways. Currently, it treats all points (i.e. all trees in the example) equally, irrespective of their properties (i.e. sizes). A refined approach could additionally consider marked points patterns and hence weight edges in the graph by tree size or a similar suitable quantity (Vuorinen et al, 2004) so that information on biomass is incorporated as well (Law et al, 2009). The approach may also be improved further by taking account of spatial heterogeneity resulting from environmental variation. This might involve simply using point level information to generate a continuous map of the diversity values over the region (a method called regionalisation, Illian et al 2008) and analysing the map using geostatistical tools.

7 Software

An R-package `spatialsegregation` for calculating exposure measures with different neighbourhoods is available at the Comprehensive R Archive Network `CRAN`.

Acknowledgements The research was funded by the Finnish graduate school of Computations and Mathematical Sciences (COMAS), a grand from the Finnish Academy of Science and Letters and Academy of Finland (project No. 111156). The authors would like to thank A. Penttinen for helpful comments and the supervision of the research.

The BCI forest dynamics research project was made possible by National Science Foundation grants to Stephen P. Hubbell: DEB-0640386, DEB-0425651, DEB-034 6488, DEB-012 9874, DEB-00753102, DEB-

9909347, DEB-961 5226, DEB-961 5226, DEB-940 5933, DEB-922 1033, DEB-9100058, DEB-8906869, DEB-8605042, DEB-8206992, DEB-7922197, support from the Center for Tropical Forest Science, the Smithsonian Tropical Research Institute, the John D. and Catherine T. MacArthur Foundation, the Mellon Foundation, the Celera Foundation, and numerous private individuals, and through the hard work of over 100 people from 10 countries over the past two decades. The plot project is part the Center for Tropical Forest Science, a global network of large-scale demographic tree plots.

References

Aguirre O, Hui G, von Gadow K, Jiménez J (2003) An analysis of forest structure using neighbourhood-based variables. For Ecol Manage 183:137–145

Baddeley A (1998) Spatial sampling and censoring. In: Barndorff-Nielsen O, Kendall W, van Lieshout M (eds) Stochastic geometry, likelihood and computation, Chapman & Hall

Baddeley AJ, van Lieshout MNM (1995) Area-interaction point processes. Ann Inst Stat Math 47(4):601–619

Bossdorf O, Schurr F, Schumacher J (2000) Spatial patterns of plant association in grazed and ungrazed shrublands in the semi-arid karoo, south africa. J Veg Sci 11(2):253–258

Buckland S, Magurran A, Green R, Fewster R (2005) Monitoring change in biodiversity through composite indices. Philos Trans R Soc B-Biol Sci 28(360):243–254

Cardinale B, Nelson K, Palmer M (2000) Linking species diversity to the functioning of ecosystems: On the importance of environmental context. Oikos (91):175–183

Ceyhan E (2009) Overall and pairwise segregation tests based on nearest neighbor contingency tables. Comput Stat Data Anal 53:2786–2808

Clark P, Evans F (1954) Distance to nearest neigbor as a measure of spatial relationships in populations. Ecology 35:445–453

Condit R (1998) Tropical forest cencus plots. Springer-Verlag

Condit R, et al (2000) Spatial patterns in the distribution of tropical tree species. Science 288:1414–1418

Dixon P (1994) Testing spatial segregation using a nearest-neighbor contingency table. Ecology 75(7):1940–1948

Hill MO (1973) Diversity and evenness: A unifying notation and its consequences. Ecology 54(2):427–432

Hubbell S, Foster R, O'Brien S, Harms K, Condit R, Wechsler B, Wright S, de Lao SL (1999) Light gap disturbances, recruitment limitation, and tree diversity in a neotropical forest. Science 283:554–557

Hubbell S, Ahumada J, Condit R, Foster R (2001) Local neighborhood effects on long-term survival of individual trees in a neotropical forest. Ecol Res (16):859–875

Hubbell S, Condit R, Foster R (2005) Barro Colorado forest census plot data. URL http://www.ctfs.si.edu/datasets/

Illian J, Penttinen A, Stoyan H, Stoyan D (2008) Statistical analysis and modelling of spatial point patterns. Statistics in practice, Wiley

Law R, Dieckmann U (2000) A dynamical system for neighbourhoods in plant communities. Ecology (81):2137–2148

Law R, Illian J, Burslem D, Gratzer G, Gunatilleke CVS, Gunatilleke IAUN (2009) Ecological information from spatial patterns of plants: insights from point process theory. J Ecol 97:616–628

Lewandowski A, Pommerening A (1997) Zur Beschreibung der Waldstruktur – Erwartete und beobachtete Arten-Durchmischung. Forstwiss Centralbl 116:129–139

Loreau M, Naeem S, Inchausti P, Bengtsson J, Grime J, Hector A, Hooper DU, Huston MA, Raffaelli D, Schmid B, Tilman D, Wardle DA (2001) Biodiversity and ecosystem functioning: current knowledge and future challenges. Science (294):804–808
Magurran A (1988) Ecological diversity and its measurement. Princeton univ. press
Magurran A (2004) Measuring biological diversity. Blackwell Publishing
Mahdi A, Law R (1987) On the spatial organization of plant species in a limestone grassland community. J Ecol 75:259–476
Marchette DJ (2004) Random graphs for statistical pattern recognition. Wiley
McGill BJ, Etienne RS, Gray JS, et al (2007) Species abundance distributions: moving beyond single prediction theories to integration within an ecological framework. Ecol Lett 10:995–1015
Møller J, Waagepetersen RP (2003) Statistical inference and simulation for spatial point processes. Chapman & Hall/CRC
Møller J, Waagepetersen RP (2007) Modern statistics for spatial point processes. Scand J Stat 34(4):643–684
Morlon H, Chuyong G, Condit R, Hubbell S, Kenfack D, Duncan T, Valencia R, Green J (2008) A general framework for the distance-decay of similarity in ecological communities. Ecol Lett (11):904–917
Motz K, Sterba H, Pommerening A (2010) Sampling measures of tree diversity. For Ecol Manage 260:1985–1996
Okabe A, Boots B, Sugihara K, Chiu SN (2000) Spatial Tessellations: Concepts and Applications of Voronoi Diagrams. Wiley
Pielou EC (1961) Segregation and symmetry in two-species populations as studied by nearest neighbour relationships. J Ecol 49(2):255–269
Pielou EC (1977) Mathematical ecology. Wiley
Podani J, Czaran T (1997) Individual-centered analysis of mapped point patterns representing multi-species assemblages. J Veg Sci 8(2):259–270
Reardon S, O'Sullivan D (2004) Measures of spatial segregation. Sociological methodology 34:121–162
Ripley BD (1977) Modelling spatial patterns. J R Stat Soc Ser B-Stat Methodol 39:172–212
Scheiner S (2003) Six types of species-area curves. Glob Ecol Biogeogr 12(6):441–447
Shimatani K (2001) Multivariate point processes and spatial variation of species diversity. For Ecol Manage 142:215–229
Shimatani K, Kubota Y (2004) Quantitative assessment of multispecies spatial pattern with high species diversity. Ecol Res 19:149–163
Stoyan D, Kendall WS, Mecke J (1995) Stochastic geometry and its applications, 2nd ed. Wiley
Tóthmérész B (1995) Comparison of different methods for diversity ordering. J Veg Sci 6:283–290
Tscheschel A, Stoyan D (2006) Statistical reconstruction of random point patterns. Comput Stat Data Anal (51):859–871
Vuorinen V, Peltomäki M, Rost M, Alava M (2004) Networks in metapopulation dynamics. Eur Phys J B 38:261–268
Waagepetersen RP, Guan Y (2009) Two step estimation for inhomogeneous spatial point processes and a simulation study. J R Stat Soc Ser B-Stat Methodol 71:685–702
Wiegand T, Gunatilleke CVS, Gunatilleke IAUN, Huth A (2007) How individual species structure diversity in tropical forests. PNAS

A Values under complete spatial randomness (CSR)

Under CSR we have for all the discussed graphs

$$\overline{\delta}_\tau = \mathbf{E}_o \sum_{x_i \in X \setminus o} \mathbf{1}(o \to x_i, t(x_i) = \tau) = \mathbf{E}_o \sum_{x_i \in X_\tau \setminus o} \mathbf{1}(o \to x_i) \quad = \quad p_\tau \cdot \overline{\delta},$$

and

$$\overline{\delta}_= = \mathbf{E}_\tau \big[\mathbf{E}_o \delta_\tau \mid t(o) = \tau \big] = \sum_{\tau=1}^{S} \mathbf{P}(t(o) = \tau) \cdot p_\tau \cdot \overline{\delta} \quad = \quad \overline{\delta} \sum_{\tau=1}^{S} p_\tau^2.$$

Moreover $\overline{\delta}_{-\tau} = \overline{\delta} - \overline{\delta}_\tau$ and $\overline{\delta}_{\neq} = \overline{\delta} - \overline{\delta}_=$. Further implication of the independence is $\overline{\delta}_{\tau,\gamma} = \overline{\delta}_\gamma$, so $\overline{\delta}_{\tau,\neq} = \overline{\delta}_{\tau,\mathscr{S}} - \overline{\delta}_{\tau,\tau} = \overline{\delta} - \overline{\delta}_\tau$. When there is no spatial structure the local proportions reduce to

$$\begin{aligned} \pi_\tau = \pi_{\tau,\tau} &= p_\tau, \\ \pi_= &= \sum_{\tau=1}^{S} p_\tau^2, \end{aligned}$$

furthermore $\pi_\tau = 1 - \pi_{-\tau}$ and $\pi_{\neq} = 1 - \pi_=$.

A.1 Measures under CSR

Spatial Simpson index:

$$\alpha(\theta) := 1 - \sum_{\tau=1}^{S} p_\tau \frac{\overline{\delta}_{\tau,\tau}}{\overline{\delta}} = 1 - \sum_{\tau=1}^{S} p_\tau \pi_\tau = 1 - \sum_{\tau=1}^{S} p_\tau^2.$$

Mingling index:

$$M_\tau(\theta) = \frac{\overline{\delta} - \overline{\delta}_\tau}{\overline{\delta}} = \frac{\overline{\delta}(1 - \frac{\lambda_\tau}{\lambda})}{\overline{\delta}} = 1 - \frac{\lambda_\tau}{\lambda}.$$

ISAR: By the independence between points and independence between types

$$\mathbf{P}_{o,\tau}(\delta_\gamma(o) = 0) = e^{-\overline{\delta} p_\gamma}$$

for any τ, so

$$\beta_\tau(\theta) = \sum_{\gamma=1}^{S} (1 - e^{-\overline{\delta} p_\gamma}).$$

ISAR depends on the graph structure and hence potentially on the parameters θ of the graphs if parameterized graphs are considered.

B Simulation algorithm for Example 1

The simulation algorithm for multitype patterns with varying scattering and exposure effects was based on a Gibbs model combining the Area-Interaction model of Baddeley and van Lieshout (1995) and the reconstruction method of Tscheschel and Stoyan (2006). The model is

$$f(X) \propto \exp\big[-a \sum_{\tau=1}^{S} A_\tau(X) - b \sum_{i=1}^{3} F_i(X) \big]$$

with $A_\tau(X) = |\bigcup_{x_i \in X_\tau} B(x_i, R)|$ being the intra-type Area-interaction point process component for the scattering effect, and the exposure effect being given by the minimum contrast components

$$\begin{aligned} F_1(X) &= (\alpha(\theta; X) - \alpha^0)^2 \\ F_2(X) &= \sum_{\tau=1}^{S} (\beta_\tau(\theta; X) - \beta_\tau^0)^2 \\ F_3(X) &= \sum_{\tau=1}^{S} (M_\tau(\theta; X) - M_\tau^0)^2 \end{aligned}$$

with estimated value for each pattern X denoted by writing it as a parameter, and the target values denoted by superscript 0.

We think that the circular use of the exposure measures in simulation of the pattern of which the measures themselves are to be calculated from is a minor problem as the focus of the example is on the effect of neighbourhood definition and how the change of it affects the measure values. Furthermore, the main interest is how the typically used geometric neighbourhood works in comparison to the others. That is why we chose a fixed geometric neighbourhood for the calculation of the contrast functions, the value $R = \frac{1.1}{\sqrt{\lambda}}$ as the constant range scaling with the number of points.

The parameters were chosen by trial runs and visual inspection to produce patterns like in the Figure 3. Clustering levels were comfirmed with pair correlation function checks. Area-interaction radius was scaled with richness, $R = \frac{1}{\sqrt{6S}}$. scattering factors varied depending on sample size and exposure. In order (clustering, no effect, regular): For small samples and mingled category $a = (50, 0, -200)$, no exposure effect $a = (300, 0, -100)$, and segregated $a = (100, 0, -100)$. For medium samples mingled $a = (50, 0, -8 \cdot 10^6)$, no exposure effect $a = (300, 0, -1200)$, and segregated $a = (100, 0 - 1200)$. The large number in regular-mingled was necessary to keep the pattern from clustering due to mingling effect. The exposure factors where in order (mingling, no effect, segregation) for both sample sizes: clustered $b = (2, 0, 5)$, no effect $b = (5, 0, 5)$, regular $b = (5, 0, 6)$.

C Tables and additional figures

Table C.1 Abundance vectors used in the simulation trials of Section 4.

	"Small richness", $S = 4$	"Medium richness", $S = 30$
Completely even	10, 10, 10, 10	$\{10\} \times 30$
Medium evenness	5, 8, 11, 16	6, 6, 7, 7, ..., 18, 18
Dominated	5, 5, 5, 25	$\{5\}\times 16$, $\{8\}\times 8$, 10, 10, 15, 15, 20, 90.

Table C.2 Results for the significance tests for low richness, with $S = 4, n = 40$. The separation of different exposure categories is based on empirical summary distributions. Each distribution is derived from 100 simulations of each of the 9 point classes using the Delaunay and the Gabriel neighbourhood. The sample distributions of each of the three summary charactistics are compared, one for each of the three exposure levels and for each different type of neighbourhood, level of evenness and scattering. The results are coded as ▽ Segregated vs. no effect; △ no effect vs. mingled; ◊ segregated vs. mingled. A filled symbol indicates significance at the 5%-level (Mann-Whitney signed rank test).

Mean mingling index

Evenness:	Completely even	Medium evenness	Dominated
Scattering:	Clust.|No effect|Regular	Clust.|No effect|Regular	Clust.|No effect|Regular
Delaunay	▼▲◆|▼▲◆|▼ △ ◆	▼▲◆|▼▲◆|▼ △ ◆	▼▲◆|▼▲◆|▽ △ ◊
Gabriel	▼▲◆|▼▲◆|▼ △ ◆	▼▲◆|▼▲◆|▼▲◆	▼▲◆|▼▲◆|▽ △ ◊

Spatial Simpson index

Evenness:	Completely even	Medium evenness	Dominated
Scattering:	Clust.|No effect|Regular	Clust.|No effect|Regular	Clust.|No effect|Regular
Delaunay	▼▲◆|▼▲◆|▼ △ ◆	▼▲◆|▼▲◆|▼▲◆	▼▲◆|▼▲◆|▽ △ ◊
Gabriel	▼▲◆|▼▲◆|▼ △ ◆	▼▲◆|▼▲◆|▼▲◆	▽▲◆|▼▲◆|▽▲◊

Mean ISAR

Evenness:	Completely even	Medium evenness	Dominated
Scattering:	Clust.|No effect|Regular	Clust.|No effect|Regular	Clust.|No effect|Regular
Delaunay	▼▲◆|▼▲◆|▽ △ ◊	▼▲◆|▼▲◆|▽ △ ◊	▼▲◆|▽▲◆|▽ △ ◊
Gabriel	▼▲◆|▼ △ ◊|▽ △ ◊	▼▲◆|▽▲◊|▽ △ ◊	▼▲◆|▽▲◊|▽ △ ◊

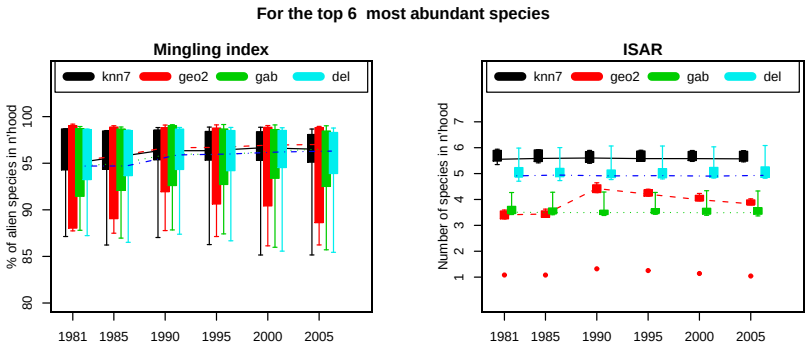

Fig. C.1 Boxplots of mingling index (left) and ISAR (right) values for the top 6 abundant species in BCI samples. The four different neighbourhoods are: 7-nearest neighbours (knn7), geometric with $R = 2m$ (geo2), Gabriel (gab) and Delaunay (del).

Table C.3 Results for the significance tests for low richness, with $S = 30, n = 40$. The separation of different exposure categories is based on empirical summary distributions. Each distribution is derived from 100 simulations of each of the 9 point classes using the Delaunay and the Gabriel neighbourhood. The sample distributions of each of the three summary charactistics are compared, one for each of the three exposure levels and for each different type of neighbourhood, level of evenness and scattering. The results are coded as ▽ Segregated vs. no effect; △ no effect vs. mingled; ◊ segregated vs. mingled. A filled symbol indicates significance at the 5%-level (Mann-Whitney signed rank test).

Mean mingling index

Evenness:	Completely even	Medium evenness	Dominated
Scattering:	Clust.|No effect|Regular	Clust.|No effect|Regular	Clust.|No effect|Regular
Delaunay	▼▲◆|▼▲◆|▼▲◆	▼▲◆|▼▲◆|▼▲◆	▼▲◆|▼▲◆|▼▲◆
Gabriel	▼▲◆|▼▲◆|▼▲◆	▼▲◆|▼▲◆|▼▲◆	▼▲◆|▼▲◆|▼▲◆

Spatial Simpson index

Evenness:	Completely even	Medium evenness	Dominated
Scattering:	Clust.|No effect|Regular	Clust.|No effect|Regular	Clust.|No effect|Regular
Delaunay	▼▲◆|▼▲◆|▼▲◆	▼▲◆|▼▲◆|▼▲◆	▼▲◆|▼▲◆|▼▲◆
Gabriel	▼▲◆|▼▲◆|▼▲◆	▼▲◆|▼▲◆|▼▲◆	▼▲◆|▼▲◆|▼▲◆

Mean ISAR

Evenness:	Completely even	Medium evenness	Dominated
Scattering:	Clust.|No effect|Regular	Clust.|No effect|Regular	Clust.|No effect|Regular
Delaunay	▼▲◆|▼▲◆|▼▲◆	▼▲◆|▼▲◆|▼▲◆	▼▲◆|▽ △ ◊|▼ △ ◊
Gabriel	▽▲◆|▽ △ ◊|▽ △ ◊	▽▲◆|▽ △ ◊|▽ △ ◊	▽▲◆|▽ △ ◊|▽ △ ◊

Table C.4 Small richness, $S = 4, n = 40$. Envelope test rejection rates for different summaries and neighbourhoods on different levels of evenness/scattering. Each number is the fraction of rejected envelope tests against the hypothesis 'no exposure effect'. ▼segregation vs. no exposure effect, ▲mingling vs. no exposure effect. Higher values are darker.

Mean mingling index

Evenness:	Completely even	Medium evenness	Dominated
Scattering:	Clustered|No effect|Regular	Clustered|No effect|Regular	Clustered|No effect|Regular
Geometric	▼0.37▲1.00|▼0.99 0.02|▼0.95 0.02	0.00▲1.00|▼1.00 0.00|▼0.97 0.02	0.00▲1.00|▼1.00 0.01|▼0.94 0.20
k-nn	0.00▲1.00|▼0.98▲0.62|▼0.97 0.09	0.06▲0.99|▼1.00▲0.62|▼0.90 0.04	0.00▲1.00|▼0.93 0.27|▼0.83▲0.48

Spatial Simpson index

Evenness:	Completely even	Medium evenness	Dominated
Scattering:	Clustered|No effect|Regular	Clustered|No effect|Regular	Clustered|No effect|Regular
Geometric	▼0.64▲1.00|▼0.99 0.04|▼0.95 0.01	▼0.31▲1.00|▼1.00 0.06|▼0.94 0.04	0.11▲1.00|▼1.00▲0.74|▼0.95 0.31
k-nn	0.00▲1.00|▼0.98▲0.62|▼0.97 0.09	0.00▲1.00|▼0.99▲0.55|▼0.81 0.06	0.00▲1.00|▼0.99▲0.82|▼0.59 0.48

Mean ISAR

Evenness:	Completely even	Medium evenness	Dominated
Scattering:	Clustered|No effect|Regular	Clustered|No effect|Regular	Clustered|No effect|Regular
Geometric	▼0.72▲1.00|▼1.00▲1.00|▼1.00▲1.00	▼0.58▲1.00|▼1.00▲1.00|▼1.00▲1.00	▼0.47▲1.00|▼1.00▲1.00|▼1.00▲1.00
k-nn	0.00▲1.00|▼0.98▲0.84|▼0.91▲0.96	0.06▲1.00|▼0.96▲0.90|▼0.57▲0.79	0.00▲1.00|▼0.71▲1.00|▼0.28▲0.98

Table C.5 Medium richness, $S = 30, n \approx 300$. Envelope test rejection rates for different summaries and neighbourhoods on different levels of evenness/scattering. Each number is the fraction of rejected envelope tests against the hypothesis 'no exposure effect'. ▼segregation vs. no exposure effect, ▲mingling vs. no exposure effect. Higher values are darker.

Mean mingling index

Evenness:	Completely even			Medium evenness			Dominated		
Scattering:	Clustered	No effect	Regular	Clustered	No effect	Regular	Clustered	No effect	Regular
Geometric	▼1.00▲1.00	▼1.00▲1.00	▼1.00▲1.00	▼1.00▲1.00	▼1.00▲0.99	▼1.00▲1.00	▼1.00▲1.00	▼1.00▲0.93	▼1.00▲1.00
k-nn	▼1.00▲1.00	▼1.00▲1.00	▼1.00▲1.00	▼1.00▲1.00	▼1.00▲1.00	▼1.00▲1.00	▼0.99▲1.00	▼1.00▲1.00	▼1.00▲1.00

Spatial Simpson index

Evenness:	Completely even			Medium evenness			Dominated		
Scattering:	Clustered	No effect	Regular	Clustered	No effect	Regular	Clustered	No effect	Regular
Geometric	▼1.00▲1.00	▼1.00▲1.00	▼1.00▲1.00	▼1.00▲1.00	▼1.00▲0.99	▼1.00▲1.00	▼1.00▲1.00	▼1.00▲0.89	▼1.00▲1.00
k-nn	▼1.00▲1.00	▼1.00▲1.00	▼1.00▲1.00	▼1.00▲1.00	▼1.00▲1.00	▼1.00▲1.00	▼0.98▲1.00	▼1.00▲1.00	▼1.00▲1.00

Mean ISAR

Evenness:	Completely even			Medium evenness			Dominated		
Scattering:	Clustered	No effect	Regular	Clustered	No effect	Regular	Clustered	No effect	Regular
Geometric	▼1.00▲1.00	▼1.00▲1.00	▼1.00▲1.00	▼1.00▲1.00	▼1.00▲1.00	▼1.00▲1.00	▼1.00▲1.00	▼1.00▲1.00	▼1.00▲1.00
k-nn	▼1.00▲1.00	▼1.00▲1.00	▼1.00▲1.00	▼1.00▲1.00	▼1.00▲1.00	▼1.00▲1.00	▼0.97▲1.00	▼1.00▲1.00	▼1.00▲1.00

Table C.6 Barro Colorado Island rainforest plot, years 1981-2005: Number of plants with dbh≥1cm, number of species and aspatial Simpson index values for each year.

BCI year	1981	1985	1990	1995	2000	2005
Sample size	235304	247947	254186	243534	227210	222602
Species	307	306	306	305	304	301
Aspatial Simpson	0.9494	0.9485	0.9489	0.9493	0.9501	0.9519

Table C.7 Mean and standard deviation (in parenthesis) of differences of species-wise mingling index and ISAR values between consecutive years. Values are computed for the 92 focal species in BCI samples with abundance of dbh>10cm trees atleast 30. The four different neighbourhoods are: 7-nearest neighbours (knn7), geometric with $R = 2m$ (geo2), Gabriel (gab) and Delaunay (del).

Mingling index

	1981–1985	1985–1990	1990–1995	1995–2000	2000–2005
knn7	-0.0004 (0.0043)	-0.0011 (0.0048)	6e-04 (0.0040)	-4e-04 (0.0047)	0.0003 (0.0042)
geo2	-2.8e-05 (0.0053)	-0.0015 (0.0061)	5e-04 (0.0036)	-0.0004 (0.0045)	0.0009 (0.0050)
gab	0.0002 (0.0048)	-0.0012 (0.0051)	9.4e-05 (0.0045)	-0.0002 (0.0066)	0.0006 (0.0047)
del	0.0001 (0.0047)	-0.0009 (0.0049)	0.0005 (0.0043)	-5e-04 (0.0052)	0.0004 (0.0040)

ISAR

	1981–1985	1985–1990	1990–1995	1995–2000	2000–2005
knn7	-0.011 (0.10)	0.051 (0.12)	-0.016 (0.10)	0.014 (0.084)	-0.01 (0.11)
geo2	-0.031 (0.15)	-0.990 (0.20)	0.230 (0.15)	0.200 (0.17)	0.130 (0.18)
gab	0.0013 (0.087)	0.026 (0.11)	-0.011 (0.10)	0.0088 (0.097)	0.01 (0.11)
del	-0.027 (0.11)	0.062 (0.16)	-0.015 (0.13)	0.00076 (0.12)	-0.017 (0.15)

Table C.8 Mean and standard deviation (in parenthesis) of differences of mingling index and ISAR values between consecutive years. Values include the top 6 abundant species. The four different neighbourhoods are: 7-nearest neighbours (knn7), geometric with $R = 2m$ (geo2), Gabriel (gab) and Delaunay (del).

Mingling index

	81–85	85–90	90–95	95–00	00–05
knn7	0.000 (0.006)	-0.006 (0.004)	0.001 (0.003)	0.001 (0.005)	0.002 (0.002)
geo2	-0.002 (0.007)	-0.008 (0.011)	0.003 (0.006)	0.001 (0.005)	0.003 (0.007)
gab	0.000 (0.005)	-0.007 (0.004)	0.002 (0.002)	0.000 (0.008)	0.002 (0.005)
del	0.001 (0.004)	-0.007 (0.005)	0.001 (0.003)	0.001 (0.006)	0.001 (0.003)

ISAR

	81–85	85–90	90–95	95–00	00–05
knn7	-0.019 (0.045)	0.018 (0.031)	-0.017 (0.044)	0.001 (0.022)	0.009 (0.021)
geo2	-0.027 (0.062)	-0.865 (0.326)	0.181 (0.076)	0.182 (0.044)	0.159 (0.051)
gab	0.015 (0.031)	0.025 (0.040)	-0.026 (0.051)	0.002 (0.043)	0.001 (0.026)
del	-0.011 (0.036)	0.010 (0.050)	-0.015 (0.036)	-0.005 (0.034)	-0.021 (0.039)

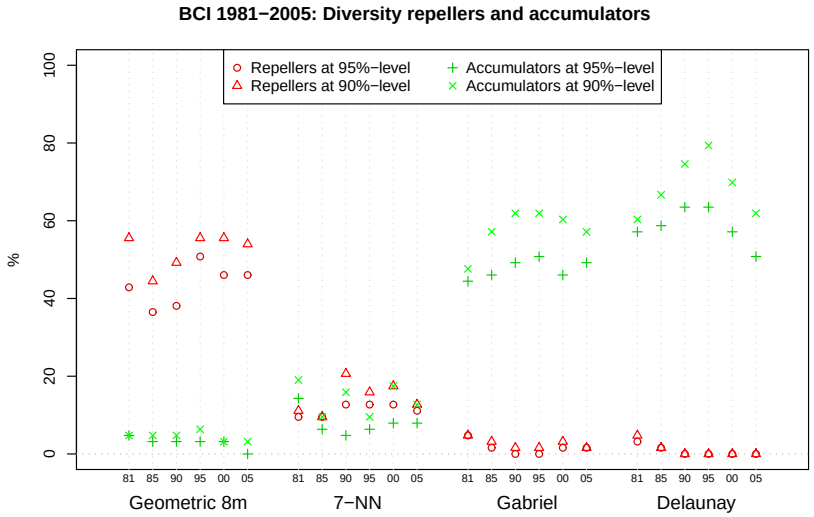

Fig. C.2 Fixed neighbourhood and diversity classification over time.